Analysis of Complement Expression in Light-Induced Retinal Degeneration: Synthesis and Deposition of C3 by Microglia/Macrophages Is Associated with Focal Photoreceptor Degeneration

Matt Rutar,[1,2] *Riccardo Natoli,*[1,3] *Peter Kozulin,*[1,2] *Krisztina Valter,*[1,2] *Paul Gatenby,*[3] *and Jan M. Provis*[1,2,3]

Purpose. To investigate the expression and localization of complement system mRNA and protein in a light-induced model of progressive retinal degeneration.

Methods. Sprague-Dawley (SD) rats were exposed to 1000 lux of bright continuous light (BCL) for up to 24 hours. At time points during (1–24 hours) and after (3 and 7 days) exposure, the animals were euthanatized and the retinas processed. Differential expression of complement genes at 24 hours of exposure was assessed using microarray analysis. Expression of complement genes was validated by quantitative PCR, and expression of selected genes was investigated during and after BCL exposure. Photoreceptor apoptosis was assessed using TUNEL and C3 was further investigated by spatiotemporal analysis using in situ hybridization and immunohistochemistry.

Results. Exposure to 24 hours of BCL induced differential expression of a suite of complement system genes, including classic and lectin components, regulators, and receptors. *C1qr1*, *MCP*, *Daf1*, and *C1qTNF6* all modulated in concert with photoreceptor death and AP-1 expression, which reached a peak at 24 hours exposure. *C1s* and *C4a* reached peak expression at 3 days after exposure, while expression of *C3*, *C3ar1*, and *C5r1* were maximum at 7 days after exposure. *C3* mRNA was detected in ED1- and IBA1-positive microglia/macrophages, in the retinal vessels and optic nerve head and in the subretinal space, particularly at the margins of the emerging lesion.

Conclusions. The data indicate that BCL induces the prolonged expression of a range of complement genes and show that microglia/macrophages synthesize *C3* and deposit it in the ONL after BCL injury. These findings have relevance to the role of complement in progressive retinal degeneration, including atrophic AMD. (*Invest Ophthalmol Vis Sci.* 2011;52:5347–5358) DOI:10.1167/iovs.10-7119

The complement system is a component of the innate immune system, which provides a rapid host defense against a range of immunologic challenges.[1,2] Through a cascade of proteolytic cleavages that generate phagocytosis-enhancing opsonins, chemotactic anaphylatoxins, and membrane-attack complexes,[3,4] the activity of this system complements the ability of the host to initiate humoral defenses against infectious pathogens[5] and promotes the removal of potentially noxious substances, including extracellular debris,[1,3,4,6] immune complexes,[2,7–9] and apoptotic cells.[8,10–13]

Despite this beneficial function, a pathogenic role of complement in age-related macular degeneration (AMD) has been uncovered through gene association studies. These identify a significant association between the Y402H sequence variant in the regulatory gene complement factor H (*CFH*) with incidence of AMD,[14–17] along with other susceptibility variants in complement pathway genes such as *C2*,[18,19] *CFB*,[18,19] and the central component *C3*.[20–24] These findings firmly establish complement activation and inflammation as factors that influence the onset and progression of AMD. Furthermore, histologic analyses of AMD donor eyes show that complement components and regulatory proteins are present in drusen,[18,25,26] suggestive of chronic complement activation. However, several key aspects of the disease process remain unclear, including the cellular events that promote complement activity in the retina.[18]

Some investigations have shown that the light-mediated model of retinal degeneration in rats has pathogenic features in common with atrophic AMD,[27–31] and it has been shown that ablation of the alternative pathway gene complement factor D (*CFD*) in this model attenuates photoreceptor death.[32] To better understand the role of complement in the degenerative process, in this study we sought to investigate the transcriptional profile and spatiotemporal distribution of complement gene expression in relation to areas of photoreceptor loss in the retina after damaging light. We found that photoreceptor death is accompanied by robust expression of complement-related genes, many of which are associated with degeneration that takes place sometime after the damaging stimulus. Further, we found synthesis of *C3* in the retina by infiltrating microglia/macrophages, in spatiotemporal coincidence with photoreceptor degeneration in the atrophic lesion.

From the [1]Research School of Biology, [2]ARC (Australian Research Council) Centre of Excellence in Vision Science, and the [3]ANU Medical School, The Australian National University, Canberra, Australian Capital Territory, Australia.

Supported by the Australian Research Council Centres of Excellence Program Grant CE0561903 and the Ophthalmic Research Institute of Australia's Brenda Mitchell grant. Hybridizations to the microarray were performed by Riccardo Natoli and Krisztina Valter as part of a study led by Jonathan Stone and supported by Australian Research Council Centres of Excellence Program Grant CE0561903. The microarray expression analyses included in this article were based on the part of the raw data derived from that study, and were performed by Matt Rutar.

Submitted for publication December 21, 2010; revised March 3 and 30, 2011; accepted April 26, 2011.

Disclosure: **M. Rutar**, None; **R. Natoli**, None; **P. Kozulin**, None; **K. Valter**, None; **P. Gatenby**, None; **J. M. Provis**, None

Corresponding author: Matt Rutar, Research School of Biology, College of Medicine, Biology and Environment, RN Robertson Building (Bldg. 46), Biology Place, The Australian National University, Canberra, ACT 0200, Australia; matt.rutar@rsbs.anu.edu.au.

TABLE 1. Genetic Analysis Probes

Gene Symbol	Gene Name	Catalog	Entrez Gene ID*
C1s	Complement component 1, s subcomponent	Rn00594278_m1	NM_138900.1
CD93 (C1qr1)	CD93 molecule (Complement component 1, q subcomponent receptor 1)	Rn00584525_g1	NM_053383.1
C1qtnf6	C1q and tumor necrosis factor related protein 6	Rn01504712_m1	NM_001034932.1
C3	Complement component 3	Mm00437858_m1	NM_009778.2
C3ar1	Complement component 3a receptor 1	Rn00583199_m1	NM_032060.1
C4b	Complement component 4, gene 1 (C4B)	Rn00709527_m1	NM_031504.2
C5r1	Complement component 5a receptor 1	Rn02134203_s1	NM_053619.1
CD55 (Daf1)	CD55 molecule (Decay accelerating factor 1)	Rn00709472_m1	NM_022269.2
GAPDH	Glyceraldehyde-3-phosphate dehydrogenase	Rn99999916_s1	NM_017008.3
Jun (AP-1)	Jun oncogene (transcription factor AP-1)	Rn99999045_s1	NM_021835.3

* National Center for Bioechnology Information, National Institutes of Health, Bethesda MD. http://www.ncbi.nlm.nih.gov/sites/gene.

METHODS

Animals and Light Exposure

All experiments conducted were in accordance with the ARVO Statement for the Use of Animals in Ophthalmic and Vision Research. Sprague-Dawley (SD) rats aged from 130 to 160 postnatal days were exposed to bright continuous light (BCL) at 1000 lux according to protocols described previously.[28] The animals were exposed to BCL for a period of 1, 3, 6, 12, 17, or 24 hours, after which time retinal tissue was obtained for analysis. Some animals were returned to dim-light (5 lux) conditions immediately after 24 hours of BCL for a period of 3 or 7 days, to assess postexposure effects. Age-matched, dim-reared animals served as control samples.

Tissue Collection and Processing

Animals were euthanatized by overdose of barbiturate administered by an intraperitoneal injection (60 mg/kg bodyweight; Valabarb; Virbac Animal Health, Regents Park, NSW, Australia). The left eye from each animal was marked at the superior surface for orientation and then enucleated and processed for cryosectioning, and the retina from the right eye was excised through a corneal incision and prepared for RNA extraction.

Eyes for cryosectioning were immediately immersion fixed in 4% paraformaldehyde in 0.1 M PBS (pH 7.3) for 3 hours at room temperature, then processed as previously described[28] and cryosectioned at 16 μm. Retinas for RNA extraction were immediately deposited in RNA stabilizer (RNAlater; Ambion, Austin, TX), prechilled on ice, and stored according to the manufacturer's instructions. RNA was then extracted from each sample according to a methodology established previously.[33] Isolated total RNA was analyzed for quantity and purity with a spectrophotometer (ND-1000; Nanodrop Technologies, Wilmington, DE), and samples with a 260/280 ratio greater than 1.90 were considered sufficient. The RNA quality in each sample was assessed (2100-Bioanalyzer; Agilent Technologies, Santa Clara, CA) where only samples with an integrity number (RIN) of $\geq$8 were used.

Microarray Experimentation and Analysis

Microarray analysis was performed using raw microarray data derived from a previous study conducted by members of our group, using rat gene microarrays (Rat Gene 1.0 ST; Affymetrix, Santa Clara, CA).[34] The full set of microarray data has been deposited in the NCBI Gene Expression Omnibus repository under accession number GSE22818 (National Center for Biotechnology Information, National Institutes of Health, Bethesda, MD). The analysis compared samples from dim-reared and 24-hour BCL experimental groups ($n = 3$ for each). The microarray data were analyzed (Partek Genomics Suite 6.4 software; Partek Inc., St. Louis, MO), and CEL files (Affymetrix) were imported into the software with background correction, normalization, and summarization, using the robust multiarray average (RMA) algorithm adjusted for probe sequence and GC content (GC-RMA). The processed values were displayed as individual probe sets representing exonic coding sequences, which were log-transformed using base 2. Differential expression analysis was performed using the analysis of variance (ANOVA) statistic with significance level of $P < 0.05$.

The heterogeneity of the resulting differential expression data was evaluated with agglomerative hierarchical clustering, using the Euclidean distance metric and principle component analysis (PCA; both provided by the Genomics Suite; Partek). The differential expression data were then clustered according to biological process as described by the Gene Ontology Consortium,[35] using functional analysis with Gene Ontology (GO) enrichment provided by the software (Partek GS Genomics Suite).[36] After this, the list of differentially expressed genes was screened for those relating to the complement cascade, using a differential expression cutoff of >50% and aided by pathway information summarized from the Gene Ontology Consortium[35] and gene grouping from the HUGO Gene Nomenclature Committee.[37]

Quantitative Real-Time Polymerase Chain Reaction

First-strand cDNA synthesis was performed as described previously.[33] Gene amplification was measured using either commercially available hydrolysis probes (*Taq*Man; Applied Biosystems, Inc. [ABI], Foster City, CA) or SYBR Green with custom designed primers, the details of which are provided in Tables 1 and 2, respectively. The hydrolysis probes were applied according to a previously established qPCR protocol.[33] The primers for SYBR Green qPCR (Table 2) were designed within a coding domain sequence transversing an intron using the Primer3 web-based design program.[38] The qPCR was performed using a commercial qPCR system (StepOnePlus; ABI). The amplification for each biological sample was performed in experimental triplicate, with the mean C_q (quantitation cycle) value then used to determine the ratio of change in expression. For both qPCRs (*Taq*man and SYBR Green; ABI), the percentage change compared to dim-reared samples was determined using the $^{\Delta\Delta}C_q$ method. The expression of the target gene was normalized to the expression of the reference gene glyceralde-

TABLE 2. qRT-PCR Custom Primer Sets

Gene Symbol	NCBI RefSeq	Forward Primer (5′–3′)	Reverse Primer (5′–3′)
CD46 (MCP)	NM_019190.1	CTCTTGGGAGCCCTCTATCC	ATTCCTTCACGGGGACTAGG
GAPDH	NM_017008.3	CCTGGAGAAACCTGCCAAG	CCTCAGTGTAGCCCAGGATG

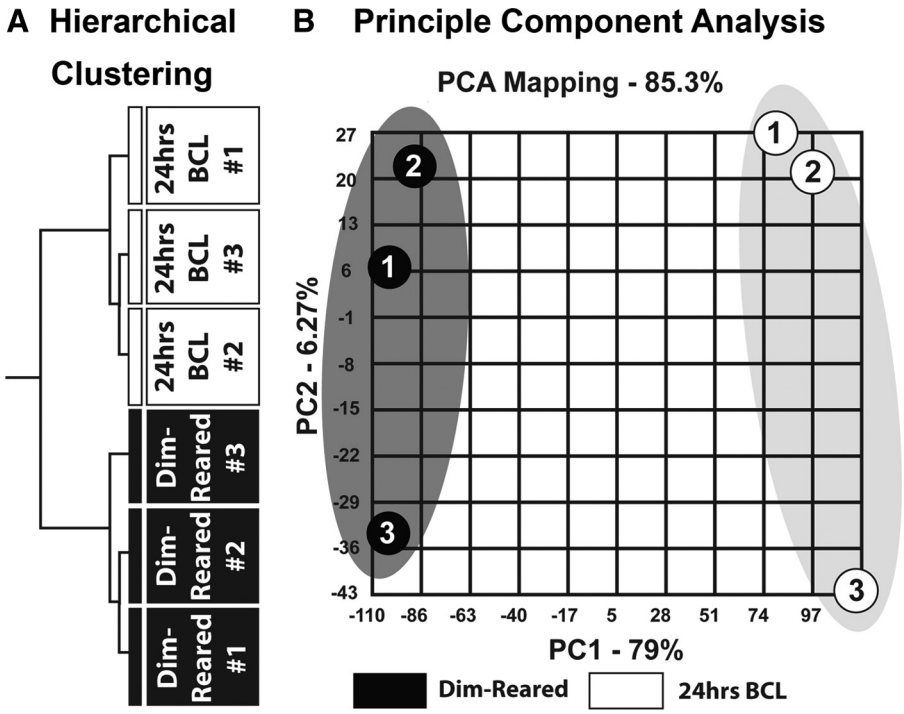

FIGURE 1. Hierarchical clustering and PCA of the processed microarray gene expression data. (**A**) Hierarchical clustering data show that sample replicates clustered closely according to their condition, either dim-reared or 24 hours of BCL. (**B**) PCA analysis, where each *circle* represents a sample replicate, showed a strong aggregation of replicates for their condition across PC1 (*x*-axis), which explains the most of the variance (79%).

hyde-3-phosphate dehydrogenase (*GAPDH*), which showed no differential expression in the present study or in previous light-induced retinal damage investigations.[32,39] Amplification specificity was assessed using gel electrophoresis. Statistical analysis was performed using the one-way ANOVA, to assess the significance of the trend in expression. Differences with a $P < 0.05$ were considered statistically significant.

In Situ Hybridization

To investigate the localization of *C3* mRNA transcripts in the retina after BCL, a riboprobe to *C3* was generated for in situ hybridization on retinal cryosections. *C3* was cloned from a PCR product (483-bp amplicon) using cDNA prepared from rat retinas (as described above), the pGEM-T DNA vector system (Promega, Madison, WI), and TOP10 competent cells (One Shot; Invitrogen). A DIG RNA-labeling kit (SP6/T7; Roche, Basel, Switzerland) was used to transcribe linearized plasmid and generate DIG-labeled antisense and sense riboprobes. In situ hybridization was performed with a protocol described previously[40]; the *C3* riboprobe was hybridized overnight at 57°C, and then washed in saline sodium citrate (pH 7.4) at 60°C. After hybridization, some sections were further stained immunohistochemically (described later).

Analysis of Cell Death

TUNEL labeling was used to quantify photoreceptor apoptosis in cryosections, during and after BCL, with a protocol published previously.[41] Counts of TUNEL-positive cells in the outer nuclear layer (ONL) were performed along the full-length of retinal sections cut in the parasagittal plane (superioinferior), including the optic disc, in adjacent fields measuring 1000 × 1000 μm. The final count from each animal is the average at comparable locations in two nonsequential sections. Statistical analysis was performed by using one-way ANOVA. Differences with a $P < 0.05$ were considered statistically significant.

Immunohistochemistry

Cryosections from each time point were used for immunohistochemical analysis, using primary antibodies for complement C3 (1:50; Abcam, Cambridge, MA), C3d (1:100; R&D Systems, Minneapolis, MN), ED1 (1:200; Millipore, Billerica, MA), and IBA1 (1:1000; Wako, Osaka, Japan). Immunohistochemistry was performed using a methodology previously described.[33] Immunofluorescence was viewed with a laser scanning microscope (Carl Zeiss Meditec, Inc.) and acquired using PASCAL software (ver. 4.0; Carl Zeiss Meditec, Inc.). Images were enhanced for publication (Photoshop; Adobe, San Jose, CA), which was standardized between images.

RESULTS

Microarray Analysis

Analysis of microarray data compared gene expression in retinas of animals reared in dim-light conditions with those exposed to 24 hours of BCL. We compiled a list of differentially expressed gene probe sets ($P < 0.05$) after BCL. Hierarchical clustering dendrograms (Fig. 1A) generated from the resulting microarray data showed strong homogeneity among biological replicates for their respective conditions (dim-reared or BCL). Principle component analysis (PCA; Fig. 1B) showed that 79% of variance in gene expression among the six animals analyzed

TABLE 3. Highly Represented Clusters of Differentially Expressed Genes after BCL

Gene Ontology ID	Biological Process	Enrichment Score
GO:0050896	Response to stimulus	73.0
GO:0009987	Cellular process	50.0
GO:0032502	Developmental process	26.0
GO:0065007	Biological Regulation	26.0
GO:0016043	Cellular component organization	24.0
GO:0051234	Establishment of localization	20.0
GO:0022610	Biological adhesion	20.0
GO:0032501	Multicellular organismal process	16.0
GO:0008152	Metabolic process	15.0
GO:0040007	Growth	8.6
GO:0002376	Immune system process	6.3
GO:0044085	Cellular component biogenesis	3.2

by microarray was due to light conditions (dim-reared or BCL), showing high reproducibility in the microarray data.

A broad perspective on the differential gene expression in these animals was achieved using Gene Ontology (GO) enrichment clustering, according to biological process, from which a list of the top 12 highly represented GO clusters was generated (Table 3). The cluster with the largest enrichment score included genes involved in response to stimulus (GO:0050896). Within this cluster (data not shown), differentially expressed genes include those involved in stimulus detection (GO: 0051606); response to external, chemical, and abiotic stimuli (GO:0042221, GO:0009628, GO:0009605); stress response (GO:0006950); and immune response (GO:0006955), which in turn includes a cluster for complement activation (GO: 0006957).

Differential Expression of Complement Genes in the Retina after BCL

Screening of the list of differentially expressed genes ($P < 0.05$) for those involved in the complement cascade resulted in the identification of a total of 18 complement-related genes, with a broad range of functional roles. Of the complement activators, complement components *C1s*, *C2*, *C3*, and *C4* (*C4b*, and *C4-2*) were upregulated as a result of exposure to BCL, as well as the carbohydrate recognition molecule ficolin B of the lectin pathway. Increased expression of complement receptors was observed, including integrin genes encoding the C3 receptors CR3 (*CD18/CD11b*) and CR4 (*CD18/CD11c*), the C3 anaphylatoxin receptor *C3ar1*, and *C1qr1*. Several complement regulators were also differently expressed after exposure to

Table 4. List of Differentially Expressed Complement System Genes after 24-Hour BCL Exposure

Gene Title	Gene Symbol	% DE (Light Damaged vs, Dim Reared)	Probe Set ID*
Complement Activators (GO:0006956, GO:0006958, GO:0001867)			
Complement component 1, s subcomponent	*C1s*	170.55	10865444
		330.74	10865449
		87.38	10865443
Complement component 2	*C2*	93.51	10828172
Complement component 3	*C3*	138.55	10931755
		296.04	10931730
		133.06	10931752
Complement component 4, gene 1	*C4b*	203.91	10828234
Complement component 4, gene 2	*C4-2*	117.93	10828255
		128.73	10828256
ficolin B	*Fcnb*	152.44	10844013
		93.29	10844006
Complement Binding Receptors (GO:0001848) and Integrins (GO:0008305)			
CD93 molecule (Complement component 1, q receptor)	*CD93* (C1qr1)	96.85	10850534
		212.17	10850536
		54.98	10850535
		175.39	10850532
Complement component 3a receptor 1	*C3ar1*	51.62	10865370
integrin beta 2 (CD18) (Complement receptor 3/4)	*CD18 (Itgb2)*	84.13	10832317
integrin alpha M (CD11b) (Complement receptor 3, subunit 2)	*CD11b (Itgam)*	122.52	10711273
		202.00	10711276
		233.02	10711291
		318.97	10711272
		96.09	10711286
integrin alpha X (CD11c)	*CD11c (Itgax)*	282.41	10711305
(Complement receptor 4, subunit 2)		77.90	10711304
		126.59	10711324
		89.00	10711307
Regulators of Complement Activation (GO:0045916, GO:0001869, GO:0001971)			
alpha-2-Macroglobulin	*a2m*	121.17	10858410
		70.62	10858418
		81.77	10858426
		64.64	10858433
CD46 molecule (membrane cofactor protein)	*CD46 (MCP)*	64.55	10770837
		111.28	10770835
		87.89	10770833
CD55 molecule (decay accelerating factor)	*CD55 (Daf1)*	94.87	10767402
Complement component 4 binding protein, beta	*C4bpb*	−63.15	10767442
		−57.28	10767441
		−70.96	10767440
		−136.52	10767439
Serine (or cysteine) peptidase inhibitor, clade G, member 1 (C1NH)	*Serping1*	54.07	10846859
Complement Related Genes			
C1q and tumor necrosis factor related protein 3	*C1qtnf3*	−112.29	10813676
C1q and tumor necrosis factor related protein 6	*C1qtnf6*	62.45	10905309

* Affymetrix, Santa Clara, CA.

BCL, including increased expression of cell-surface inhibitors *Daf1 (CD55)* and *MCP (CD46)*, soluble inhibitor *SERPING1*, and *a2m*, whereas *C4bp* expression was reduced. In addition, we observed modulation in the complement-related genes *C1qTNF3* and *C1qTNF6*, which belong to the C1q/TNF-related protein (CTRP) family of adiponectin paralogs.[42] We tested the veracity of the data by analyzing the expression of eight of the complement genes listed in Table 4, using comparative qPCR. Expression of all eight genes corresponded well with the data obtained from the microarrays (Fig. 2).

Modulation of Complement-Related Gene Expression and Cell Death

We examined the temporal expression of these same eight complement genes (Fig. 2) in relation to the number of TUNEL-positive cells in the ONL and expression of the apoptosis-related gene (*Jun [AP-1]*[43]; Fig. 3). We also included the anaphylatoxin receptor *C5r1*, in addition to the receptor *C3ar1*, even though this gene was not annotated in the microarray at the time of analysis. The temporal analysis spanned time points during (1, 3, 6, 12, 17, and 24 hours) as well as after (3 and 7 days) BCL exposure. Our previous analysis shows that the postexposure time points coincide with emergence of the lesion in the area centralis.[28]

Consistent with our previous data,[33] we observed large increases in the number of TUNEL-positive nuclei in the ONL after 12 hours of BCL, progressing to a prominent peak in cell death at 24 hours of exposure (Fig. 3A). The number of TUNEL-positive nuclei decreased substantially in the postexposure period, at 3 and 7 days. We observed a significant upregulation in *AP-1* expression after 3 hours of BCL exposure, which reached peak expression at 24 hours, coincident with peak cell death and declined rapidly during the postexposure period (Fig. 3A).

Expression of complement components *C1s*, *C3*, and *C4b* (Fig. 3B) increased significantly between 12 and 24 hours of BCL, and all three components reached peak expression in the postexposure period. *C1s* and *C4a* reached peak expression at 3 days; the data do not show what happened to C3 expression after its apparent peak at 7 days. The receptor *C1qr1* reached a peak expression in conjunction with the maximum cell death and AP-1 expression, at 24 hours of BCL (Fig. 3C). In contrast, expression of the complement receptors *C3ar1* and *C5r1* reached a peak at 3 to 7 days after exposure (Fig. 3C). The present experiments do not show how prolonged the expression of these receptors might be. Expression of the complement inhibitors *MCP* and *Daf1* reached a peak at 24 hours of BCL (Fig. 3D), coincident with the peak in photoreceptor apoptosis, with *MCP* showing the earlier and more robust expression between 12 and 24 hours of exposure. *C1qTNF6* showed modest upregulation by 24 hours, followed by a gradual decrease during the postexposure period (Fig. 3D).

Spatiotemporal Analysis of C3 Expression and Immunoreactivity after BCL

Because of its pivotal role in the activation of all three complement pathways and robust long-term upregulation after BCL (Fig. 3B), we selected C3 for further characterization. Spatiotemporal analysis of *C3* expression was conducted by in situ hybridization (Fig. 4). In dim-reared animals, *C3* expression was observed in sparsely distributed nuclei associated with the superficial retinal vasculature (Fig. 4A). After 24 hours of BCL, we detected a substantial increase in these *C3*-positive cells in the retinal vasculature, which were preferentially recruited into the superior retina (Figs. 4B, 4C), where a hotspot in photoreceptor death has been described previously.[28] *C3*-expressing nuclei showed continued recruitment to the retinal vasculature in spatial correlation with the developing lesion at 3 days after exposure (Fig. 4D), and were also detected in vessels at the optic nerve head (Figs. 4E, 4F). By 7 days after exposure, *C3*-expressing cells were still present in large numbers in the retinal vasculature and optic nerve head (data not shown) and were also observed in association with the degenerative remains of photoreceptors in the superior retina (Figs. 4G, 4H). Accumulations of *C3*-expressing cells were particularly abundant within the ONL and subretinal space at the margin of the lesion by 7 days after exposure (Figs. 4J–L). Few to none of these were present in nonlesion areas of the retina at 7 days (Fig. 4I). The identity of these *C3*-expressing cells was determined with the microglia/macrophage markers IBA1 (Figs. 4M–O) and ED1 (Figs. 4Q–U). Most *C3*-expressing cells were immunoreactive (IR) for IBA1, mainly within the ONL and subretinal space associated with the lesion (Figs. 4M–O), and some with ramified morphology (Fig. 4N-O, asterisks). IR

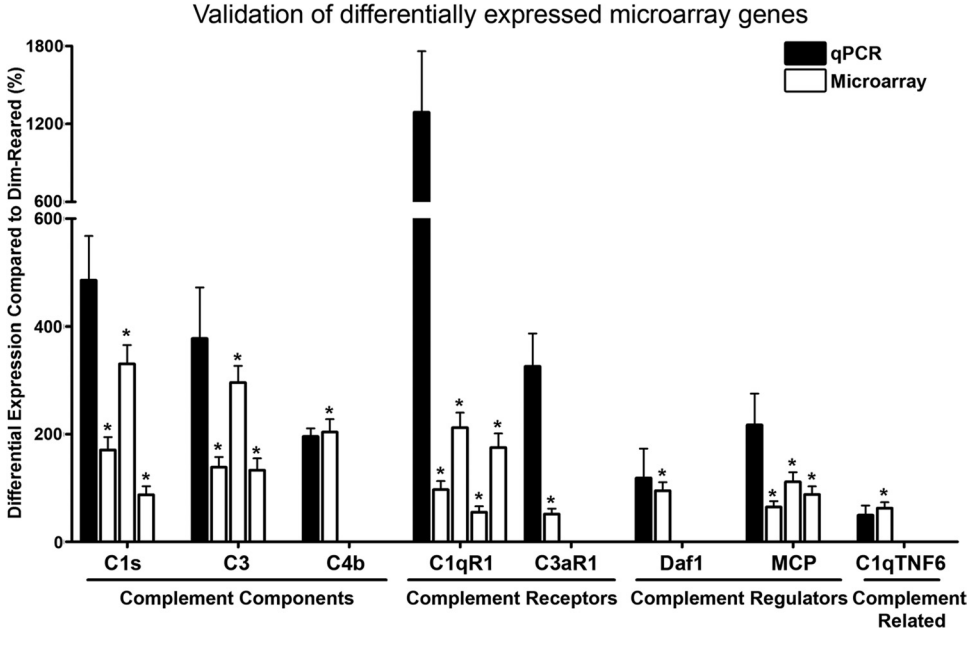

Figure 2. Comparative qPCR validation of differentially expressed genes at 24 hours of BCL. Several significantly (*probeset where $P < 0.05$) differentially expressed microarray genes were selected for comparative expression analysis using qPCR. Consistent increases were detected by qPCR for each gene, which confirmed the increases in microarray gene expression. The trends in qPCR expression were generally higher than those in the microarray, particularly for *C1qr1* and *C3ar1*.

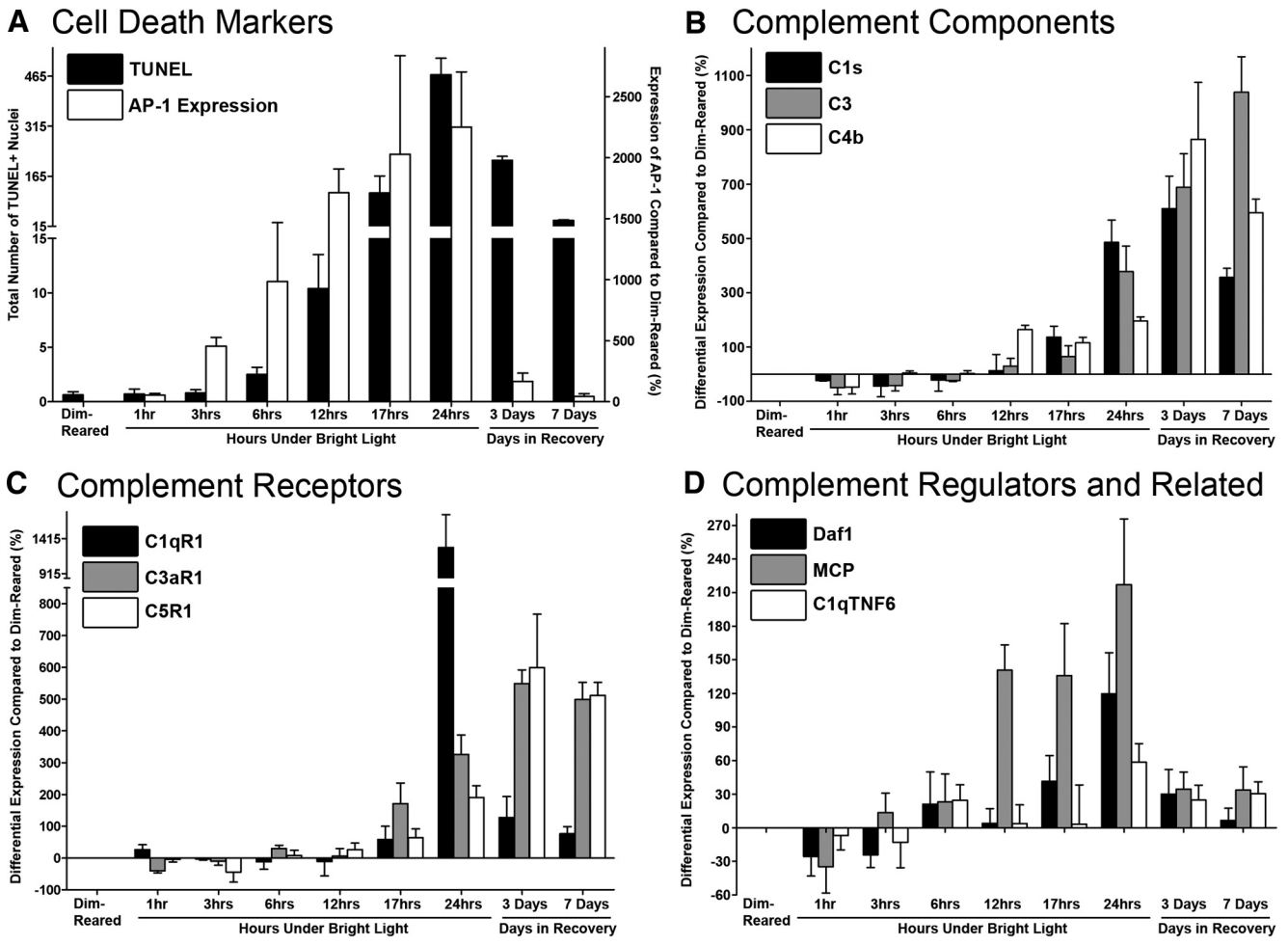

Figure 3. Expression of validated complement genes (from Fig. 2) over a protracted BCL time course in relation to cell death markers. (**A**) The frequency of TUNEL-positive nuclei in the ONL and expression of *AP-1* were used as markers of apoptosis. Increases in TUNEL were observed after 12 hours of BCL, which progressed to a peak at 24 hours. The number of TUNEL-positive nuclei decreased substantially in the postexposure period. *AP-1* increased rapidly from 3 hours of BCL onward to reach a peak at 24 hours, and then tapered off rapidly by 3 days after exposure. (**B**) Upregulation of complement components *C1s, C3*, and *C4b* occurred between 12 and 24 hours of BCL, and remained substantially upregulated, particularly C3, in the postexposure period. (**C**) Expression of complement receptors C1qr1, *C3ar1,* and *C5r1* increased substantially by 17 hours of BCL. *C3ar1* and *C5r1* continued to upregulate into the postexposure period, whereas *C1qr1* reached a considerable peak at 24 hours before falling rapidly. (**D**) *MCP* upregulated rapidly from 12 hours of BCL to reach a peak at 24 hours, whereas *Daf1* also increased over a similar time course. The complement-related gene *C1qTNF6* was found to increase slightly after 24 hours of BCL, which decreased slightly over the postexposure period. The trend in expression for all genes, as well as TUNEL, was significant by one-way ANOVA ($P < 0.05$).

for ED1 was also shown by some *C3*-expressing nuclei, such as those associated with the subretinal space in and around the lesion (Figs. 4Q–U).

IR for C3 protein was performed using antibodies against whole C3 (Figs. 5A–J), and the long-lived cleavage fragment, C3d (Fig. 5K-M).[44] C3 was detected faintly within the retinal vasculature and choroid of dim-reared animals (Fig. 5A). Similar levels of expression were detected in animals exposed to 24 hours of BCL (data not shown). However, at 3 days after exposure, we detected emerging C3-IR in the layer of outer segments at the site of the developing lesion (Fig. 5B). Areas outside the lesion were only faintly C3-IR (Fig. 5C). By 7 days after exposure, C3-IR was more intense (Figs. 5D–I) and formed multiple deposits throughout the ONL within the

Figure 4. In situ hybridization for *C3* mRNA in the retina after exposure to BCL. (**A**) In retinas from dim-reared animals, expression of *C3* was observed infrequently in nuclei associated with the superficial vasculature (*arrowhead*). (**B**, **C**) After 24 hours of BCL, *C3*-positive nuclei were preferentially recruited to the retinal vasculature in the superior retina (**B**, *arrowheads*); no such infiltration was found in the inferior (**C**). (**D**) The recruitment of *C3*-positive nuclei in the retinal vasculature continued 3 days after exposure, in association with the developing lesion (*arrowheads*). (**E**, **F**) Robust infiltration of *C3*-positive nuclei was observed in association with the optic nerve head at 3 days after exposure. (**G–I**) By 7 days after exposure, *C3*-positive nuclei had infiltrated the ONL and subretinal space within the lesion (**G**, **H**), whereas nonlesion areas in the inferior retina remained comparable to dim-reared animals (**I**). (**J–L**) Seven days after exposure a large number of *C3*-positive nuclei aggregated at the edges of the lesion. (**M–P**) *C3* expression (*dark gray*) in sections counterimmunolabeled with anti-IBA1 (*green*), showing immunoreactivity in many *C3*-expressing nuclei within the degenerating ONL (*white arrowheads*); some of these cells were ramified (✱). (**Q–U**) *C3* expression (*dark gray*) in sections counterimmunolabeled with anti-ED1 (*green*), showing immunoreactivity in some of the *C3*-expressing nuclei associated with the edge of the lesion (*white arrowheads*). C, choroid; GCL, ganglion cell layer; INL, inner nuclear layer; ONL, outer nuclear layer; S, subretinal space.

lesion area, in the subjacent subretinal space (Figs. 5D, 5E), and in segments of the retinal vasculature (Fig. 5J). On the margins of the lesion, we observed intense C3-IR in ONL deposits (Figs. 5F, 5G) and on photoreceptor outer segments (Fig. 5H, 5I), coinciding with aggregations of C3-expressing macrophages (Figs. 5J–L). IR for C3d showed spatiotemporal distribution very similar to that of whole-C3 after BCL (Figs. 5K–O). In dim-reared animals, C3d-IR was faintly detected in the choroid and retinal vasculature (Fig. 5K). By 7 days after exposure, C3d had accumulated in

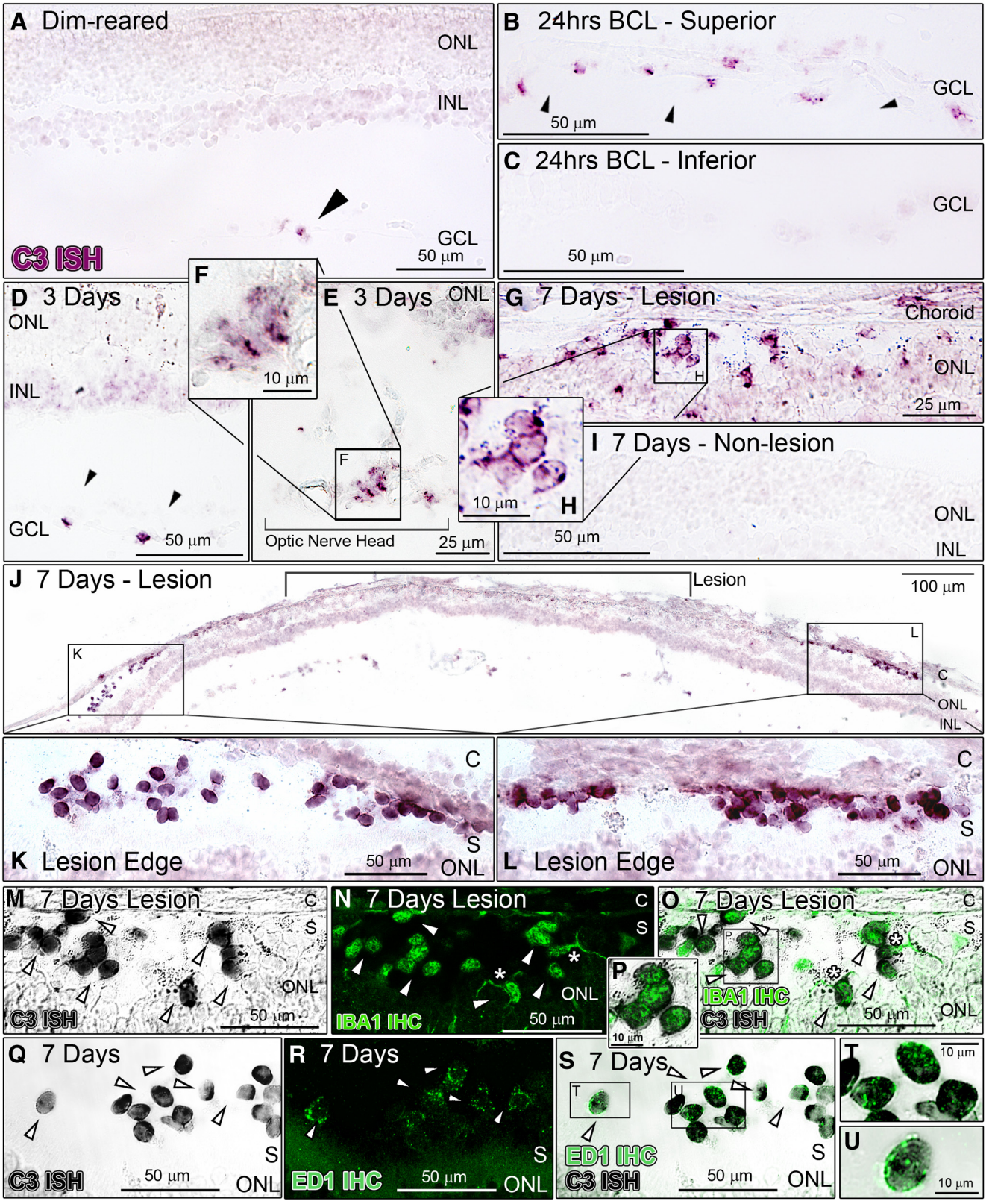

FIGURE 4.

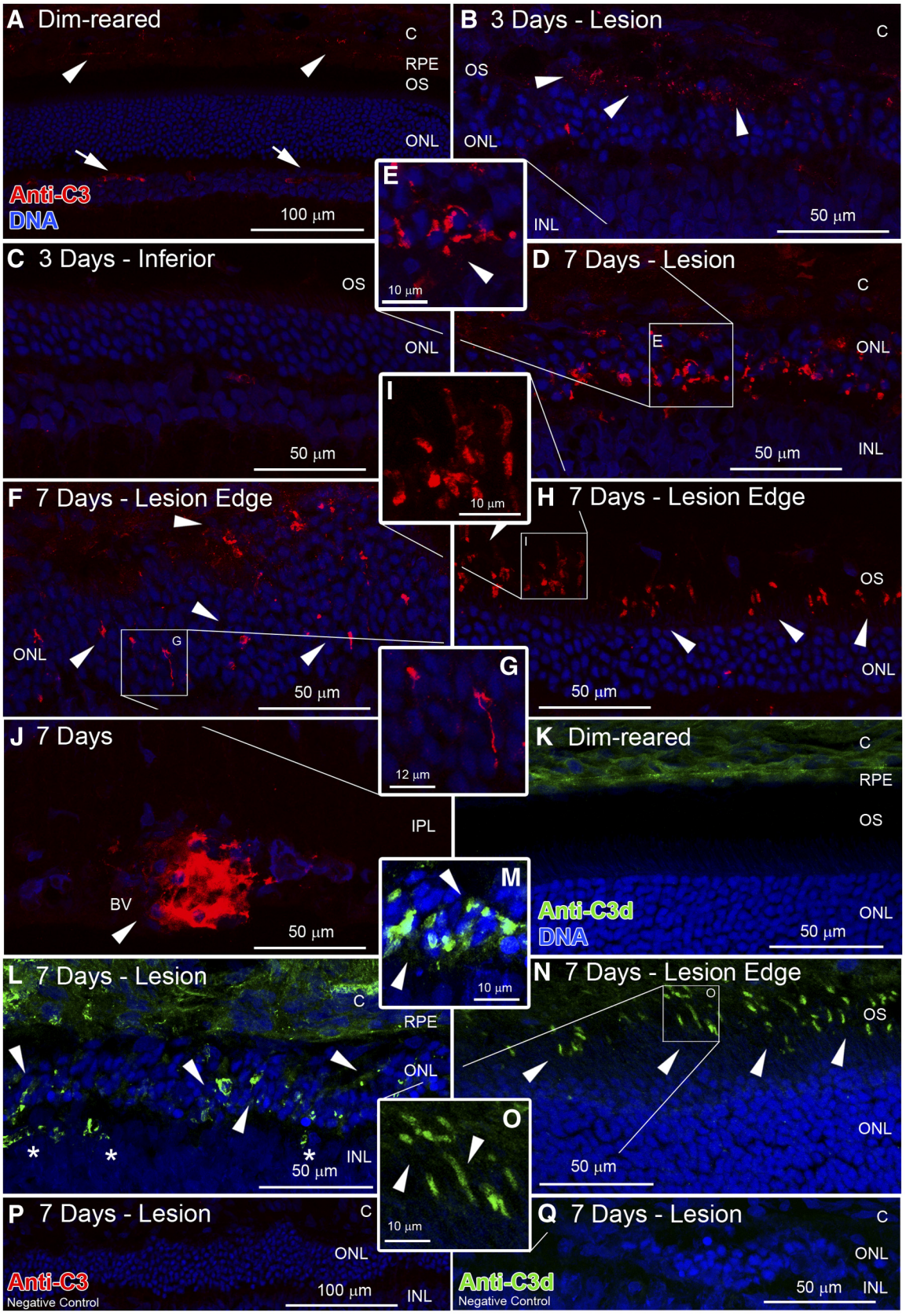
A Dim-reared
C
RPE
OS
ONL
Anti-C3
DNA
100 μm
B 3 Days - Lesion
C
OS
ONL
INL
50 μm
E
10 μm
C 3 Days - Inferior
OS
ONL
50 μm
D 7 Days - Lesion
C
E
ONL
50 μm
INL
I
10 μm
F 7 Days - Lesion Edge
ONL
G
50 μm
H 7 Days - Lesion Edge
I
OS
ONL
50 μm
G
12 μm
J 7 Days
IPL
BV
50 μm
K Dim-reared
C
RPE
OS
M
Anti-C3d
DNA
ONL
50 μm
10 μm
L 7 Days - Lesion
C
RPE
ONL
INL
50 μm
N 7 Days - Lesion Edge
O
OS
ONL
50 μm
O
10 μm
P 7 Days - Lesion
C
ONL
Anti-C3
Negative Control
100 μm
INL
Q 7 Days - Lesion
C
ONL
Anti-C3d
Negative Control
50 μm
INL

FIGURE 5.

numerous deposits situated in the ONL and subretinal space within the lesion area (Figs. 5L, 5M), in close association with photoreceptor cell bodies (Fig. 5M), and on photoreceptor outer segments at the lesion edge (Figs. 5N, 5O).

Discussion

The results of this study confirmed robust differential expression in the neural retina of several complement system genes after light-induced retinal degeneration. These data are consistent with the findings in a previous microarray study.[32] In addition, we demonstrated several key findings that elaborate on the role of complement in retinal damage induced by BCL. First, by microarray analysis and qPCR, we showed modulation of a suite of complement genes, including opsonin mediators from classic and lectin pathways (*C1s*, *C2*, *C4*, and ficolin B), complement receptors (*C1qr1*, *C3ar1*, *C5r1*, *CR3*, *CR4*), and regulators (*MCP*, *Daf1*, *SERPING1*, *C4bp*, *a2m*), many of which have not been reported previously.[32] Second, we showed the time course of modulation of some of these genes in relation to increasing levels of photoreceptor apoptosis, demonstrating persistence of upregulation beyond 24 hours of exposure—the peak of cell death (*C1s*, *C3*, *C4b*, *C3ar1*, and *C5r1*). Third, we showed that microglia/macrophages synthesize *C3* which is preferentially deposited in the ONL and layer of outer segments in the damaged region and at the margins of the lesion in the postexposure period.

Microglia Synthesize C3 and Mediate Photoreceptor Death in Damaged Retina

To our knowledge, this is the first investigation to specifically identify cells expressing *C3* in the degenerating retina and to determine the spatiotemporal profile of C3 deposition in relation to the degenerating region. In this study, we demonstrated *C3* expression by microglia/macrophages IR for IBA1 and ED1, in spatiotemporal correlation with degeneration of the superior retina and C3 deposition after exposure to BCL,[28] suggesting that these aggregating cells are responsible for the local propagation of complement in the retina after light-induced damage. The emergence of *C3*-expressing cells from within the retinal vasculature and optic nerve head, rather than the parenchyma, after BCL, suggests that *C3* is expressed initially by recruited macrophages/monocytes.[43,45] This finding is also supported by the immunoreactivity of some cells to the monocyte/macrophage marker ED-1[46] and by other studies describing the synthesis of C3 by macrophages in vitro.[47–50] Expression of *C3* was observed in both ramified and nonramified IBA1-positive cells in the subretinal space at 7 days after exposure. This late expression of *C3* by ramified cells suggests that parenchymal microglia also synthesize *C3*,[46] but are relatively slow to respond to BCL in this synthesis, compared with recruited monocytes. Our data strongly suggest that photoreceptors are a target of C3 deposition by infiltrating C3-expressing cells after BCL, as both C3 and C3d immunoreactivity was closely associated with photoreceptor cell bodies and outer segments in relation to the lesion.

The present findings suggest that retinal degeneration associated with the developing lesion is mediated at least in part by C3 deposited by *C3*-expressing microglia/macrophages. Although complement activation has beneficial properties, such as aiding in debris clearance by recruited phagocytes,[4] complement propagation has been shown to exacerbate photoreceptor death in light-induced damage,[32] of which C3 is a vital component that drives activation of all three complement pathways. C3 is also crucial to the assembly of the C5 convertase, a mediator of the MAC complex, which may induce apoptosis or necrosis of host cells.[51] Moreover, several studies have shown that microglial activation and aggregation are associated with photoreceptor degeneration in light-induced damage.[52,53] The association of microglia/macrophages at the edge of lesion also suggests a role in chronic expansion of the lesion characterized previously,[28] although the localization of *C3*-expressing microglia past 7 days after exposure is currently unknown.

A Transcriptional Profile of Complement Activation after BCL

The transcriptional profile of complement gene expression after BCL provides insight into the breadth of complement activation in this model and its likely roles in the degenerative process. First, upregulation of macrophage receptors that recognize cleavage products of C3 (*C3ar1, CR3,* and *CR4*) and C5 (*C5r1*),[54] after exposure to BCL, indicate extensive activation of complement in the neural retina with the involvement of phagocytic cells. Second, there is an apparent compensatory upregulation of complement inhibitor genes (*MCP, Daf1, SERPING1*, and *a2m*) associated with the peak in photoreceptor death. Of these, *MCP* attenuates all three complement pathways[55] and is expressed by photoreceptors.[56] Increased expression of *MCP* suggests activation of a protective mechanism by stressed photoreceptors after BCL, in an attempt to safeguard from deleterious complement activation. Third, we found increased expression of many genes involved in the clearance of apoptotic cells. Classic pathway complement components (*C1s, C2,* and *C4*), as well as the C3-fragment receptors *CR3* and *CR4*, were expressed strongly after 24 hours of BCL. This pattern of expression is consistent with a role in the removal of apoptotic cells,[1,10–13] including uptake of apoptotic cells by macrophages.[57,58] However, the ablation of *C1qα* in rd1 mice did not appear to delay the removal of apoptotic cells, indicating that the classic pathway— or at least *C1qα*—alone may not be sufficient to initiate their clearance.[59] We also showed differential expression of the carbohydrate recognition molecule ficolin B, which promotes the removal of late-stage apoptotic cells through binding to DNA,[60] mediated by the lectin pathway. Upregulation of these genes suggests that a role of complement activation in this model is the efficient removal of apoptotic cells after BCL.

Figure 5. Immunoreactivity (IR) for whole-C3 (*red*) and C3d (*green*) in the retina after exposure to BCL. (**A**) IR for C3 was faintly detected in the choroid and retinal vasculature of dim-reared retinas (*arrows* and *arrowheads*). (**B**, **C**) At 3 days after exposure C3-IR was observed in the layer of degenerating outer segments in superior retina (**B**, *arrowheads*); inferior retina was largely unreactive to C3 (**C**). (**D**, **E**) At 7 days after exposure C3-IR was intense in the ONL and subretinal space in association within the lesion. (**F–I**) At the edges of the lesion after 7 days, C3-IR was found deposited within the ONL (**F**, *arrowheads*) and in the layer of outer segments (**G**, **H**, *arrowheads*). (**J**) Portions of superficial retinal vasculature showed strong IR for C3 at 7 days after exposure. IR for C3d (**K–M**) showed a similar spatiotemporal distribution to C3. (**K**) C3d IR was faintly detected in the choroid and retinal vasculature (data not shown) of dim-reared retinas. (**L–O**) In the lesion at 7 days after exposure, C3d-IR was widespread in deposits in the ONL (*arrowheads*) and subretinal space (**L**, **M**); on the lesion edge, C3d-IR was detected on photoreceptor outer segments (**N**, **O,** *arrowheads*). (✱) Blood vessels. (**P**, **Q**) Negative controls showed no specific staining for either C3 or C3d. BV, blood vessel; C, choroid; INL, inner nuclear layer; IPL, inner plexiform layer; ONL, outer nuclear layer; OS, outer segment layer; RPE, retinal pigment epithelium; S, subretinal space.

Conversely, our findings implicate complement activation in exacerbating light-mediated retinal damage, where complement components (*C1s, C3,* and *C4*) and anaphylatoxin receptors (*C3ar1* and *C5r1*) showed persistent upregulation in the postexposure period, despite the significantly lower levels of photoreceptor death. These findings are indicative of chronic propagation of complement long after its initial activation by the damaging stimulus, and they correlate with the detrimental effect of complement demonstrated by Rohrer et al.[32] This dichotomy in the effects of complement activation has been documented previously,[54,61–63] and likely reflects a disruption of the balance between complement activation and inhibition. In light-induced damage, this may be spurred by the abundance of activating surfaces (apoptotic cells, debris) that arises after the damaging stimulus. Given that alternative pathway activation is implicated in the mediation of light-induced degeneration,[32] chronic synthesis of classic components detected in this study may stimulate further activation of complement through the amplification loop initiated by the alternative pathway,[64] as demonstrated by Rohrer et al.[65] in experimental choroidal neovascularization.

Relevance to the Role of Complement in AMD

Previous studies have shown that light-induced damage in rats has features in common with the pathogenesis of atrophic AMD.[27–31] Although the long-term features of atrophic AMD, such as pigmentary disturbance and drusen, are absent from this model, the development of a lesion aligned to the visual axis,[66] the characteristics of the lesion (which affect the photoreceptor layer, RPE and Bruch's membrane), and its progressive nature occur in common with the atrophic AMD lesion.[28] Like the widely used laser-induced model of neovascular AMD, this model employs an acute damaging stimulus to evoke long-term, site-specific changes in the retina and adjacent tissues.

The cellular events that lead to the propagation of complement in the human retina are not well understood.[18,67] Nonetheless, it is well established that polymorphisms in a range of complement-related genes is associated with risk of AMD,[18] and the high levels of association between the Y402H polymorphism of the *CFH* gene and risk of AMD[14–17] implicate failure to regulate the alternative pathway of complement activation with onset and progression of AMD. Experimental findings using the present model of retinal degeneration implicate activation of complement pathways in onset and progression of the retinal lesion, and show conclusively that microglia/macrophages express *C3*, which is deposited in the photoreceptor layer. In these conditions, photoreceptors may become the target for activation of the alternative pathway, which would culminate in the formation of MAC, cytolysis, and cytotoxic cell death.[51] Consistent with this as a mechanism in AMD, the MAC complex has been identified in drusen of donor eyes from individuals, with and without the at-risk Y402H genotypes.[68] Moreover, accumulation of microglial cells in the macula is strongly associated with AMD pathology (Wong J, et al. *IOVS* 2001;42:ARVO E-Abstract 1222).[69–73] In the atrophic form of AMD, photoreceptor and RPE degeneration on the edges of the lesion results in progressive expansion of the lesion,[74] and a recent study has shown that macrophages accumulate on the edges of AMD lesions.[75] The present findings suggest that these aggregations of macrophages are focal points of C3 synthesis and deposition, which may actively progress the elimination of photoreceptors in the vicinity, if left unchecked. Indeed, several studies that have shown an association in polymorphisms of *C3* with the progression of AMD to geographic atrophy.[21,75–77] Defects in regulatory genes, including *CFH*, may therefore predispose the photoreceptors to progressive degeneration through aberrant complement propagation induced by activated microglia/macrophages.

Conclusion

Our findings demonstrate that exposure to damaging light induces prolonged spatiotemporal changes in the expression of a suite of complement-related genes and further clarify the role of complement in the progression of retinal degeneration. Our evidence suggests that complement activation in the retina has both positive and negative effects, being beneficial to the maintenance of homeostasis after injury, yet harmful because of sustained propagation of components beyond the immediate injury and clean-up period. The synthesis of *C3* by microglia/macrophages implicates their recruitment in the local activation of complement after retinal damage. The findings therefore suggest that therapeutic attenuation of microglial recruitment may be useful strategy to control detrimental propagation of complement in the retina.

References

1. Paidassi H, Tacnet-Delorme P, Garlatti V, et al. C1q binds phosphatidylserine and likely acts as a multiligand-bridging molecule in apoptotic cell recognition. *J Immunol.* 2008;180:2329–2338.
2. Walport MJ. Complement: second of two parts. *N Engl J Med.* 2001;344:1140–1144.
3. Gasque P. Complement: a unique innate immune sensor for danger signals. *Mol Immunol.* 2004;41:1089–1098.
4. Gasque P, Dean YD, McGreal EP, VanBeek J, Morgan BP. Complement components of the innate immune system in health and disease in the CNS. *Immunopharmacology.* 2000;49:171–186.
5. Frank MM, Fries LF. The role of complement in inflammation and phagocytosis. *Immunol Today.* 1991;12:322–326.
6. Sim RB, Kishore U, Villiers CL, Marche PN, Mitchell DA. C1q binding and complement activation by prions and amyloids. *Immunobiology.* 2007;212:355–362.
7. Davies KA, Schifferli JA, Walport MJ. Complement deficiency and immune complex disease. *Springer Semin Immunopathol.* 1994; 15:397–416.
8. Botto M. C1q knock-out mice for the study of complement deficiency in autoimmune disease. *Exp Clin Immunogenet.* 1998;15: 231–234.
9. Navratil JS, Korb LC, Ahearn JM. Systemic lupus erythematosus and complement deficiency: clues to a novel role for the classical complement pathway in the maintenance of immune tolerance. *Immunopharmacology.* 1999;42:47–52.
10. Korb LC, Ahearn JM. C1q binds directly and specifically to surface blebs of apoptotic human keratinocytes: complement deficiency and systemic lupus erythematosus revisited. *J Immunol.* 1997;158: 4525–4528.
11. Taylor PR, Carugati A, Fadok VA, et al. A hierarchical role for classical pathway complement proteins in the clearance of apoptotic cells in vivo. *J Exp Med.* 2000;192:359–366.
12. Trouw LA, Blom AM, Gasque P. Role of complement and complement regulators in the removal of apoptotic cells. *Mol Immunol.* 2008;45:1199–1207.
13. Gullstrand B, Martensson U, Sturfelt G, Bengtsson AA, Truedsson L. Complement classical pathway components are all important in clearance of apoptotic and secondary necrotic cells. *Clin Exp Immunol.* 2009;156:303–311.
14. Edwards AO, Ritter R 3rd, Abel KJ, Manning A, Panhuysen C, Farrer LA. Complement factor H polymorphism and age-related macular degeneration. *Science.* 2005;308:421–424.
15. Klein RJ, Zeiss C, Chew EY, et al. Complement factor H polymorphism in age-related macular degeneration. *Science.* 2005;308: 385–389.
16. Hageman GS, Anderson DH, Johnson LV, et al. A common haplotype in the complement regulatory gene factor H (HF1/CFH)

predisposes individuals to age-related macular degeneration. *Proc Natl Acad Sci U S A.* 2005;102:7227–7232.
17. Haines JL, Hauser MA, Schmidt S, et al. Complement factor H variant increases the risk of age-related macular degeneration. *Science.* 2005;308:419–421.
18. Anderson DH, Radeke MJ, Gallo NB, et al. The pivotal role of the complement system in aging and age-related macular degeneration: hypothesis re-visited. *Prog Retin Eye Res.* 2010;29:95–112.
19. Jakobsdottir J, Conley YP, Weeks DE, Ferrell RE, Gorin MB. C2 and CFB genes in age-related maculopathy and joint action with CFH and LOC387715 genes. *PLoS One.* 2008;3:e2199.
20. Spencer KL, Olson LM, Anderson BM, et al. C3 R102G polymorphism increases risk of age-related macular degeneration. *Hum Mol Genet.* 2008;17:1821–1824.
21. Park KH, Fridley BL, Ryu E, Tosakulwong N, Edwards AO. Complement component 3 (C3) haplotypes and risk of advanced age-related macular degeneration. *Invest Ophthalmol Vis Sci.* 2009; 50:3386–3393.
22. Maller JB, Fagerness JA, Reynolds RC, Neale BM, Daly MJ, Seddon JM. Variation in complement factor 3 is associated with risk of age-related macular degeneration. *Nat Genet.* 2007;39:1200–1201.
23. Yates JR, Sepp T, Matharu BK, et al. Complement C3 variant and the risk of age-related macular degeneration. *N Engl J Med.* 2007; 357:553–561.
24. Despriet DD, van Duijn CM, Oostra BA, et al. Complement component C3 and risk of age-related macular degeneration. *Ophthalmology.* 2009;116:474–480 e472.
25. Donoso LA, Kim D, Frost A, Callahan A, Hageman G. The role of inflammation in the pathogenesis of age-related macular degeneration. *Surv Ophthalmol.* 2006;51:137–152.
26. Hageman GS, Luthert PJ, Victor Chong NH, Johnson LV, Anderson DH, Mullins RF. An integrated hypothesis that considers drusen as biomarkers of immune-mediated processes at the RPE-Bruch's membrane interface in aging and age-related macular degeneration. *Prog Retin Eye Res.* 2001;20:705–732.
27. Marc RE, Jones BW, Watt CB, Vazquez-Chona F, Vaughan DK, Organisciak DT. Extreme retinal remodeling triggered by light damage: implications for age related macular degeneration. *Mol Vis.* 2008;14:782–806.
28. Rutar M, Provis JM, Valter K. Brief exposure to damaging light causes focal recruitment of macrophages, and long-term destabilization of photoreceptors in the albino rat retina. *Curr Eye Res.* 2010;35:631–643.
29. Sullivan R, Penfold P, Pow DV. Neuronal migration and glial remodeling in degenerating retinas of aged rats and in nonneovascular AMD. *Invest Ophthalmol Vis Sci.* 2003;44:856–865.
30. Marco-Gomariz MA, Hurtado-Montalban N, Vidal-Sanz M, Lund RD, Villegas-Perez MP. Phototoxic-induced photoreceptor degeneration causes retinal ganglion cell degeneration in pigmented rats. *J Comp Neurol.* 2006;498:163–179.
31. Wielgus AR, Collier RJ, Martin E, et al. Blue light induced A2E oxidation in rat eyes - experimental animal model of dry AMD. *Photochem Photobiol Sci.* 2010;9:1505–1512.
32. Rohrer B, Guo Y, Kunchithapautham K, Gilkeson GS. Eliminating complement factor D reduces photoreceptor susceptibility to light-induced damage. *Invest Ophthalmol Vis Sci.* 2007;48:5282–5289.
33. Rutar M, Natoli R, Valter K, Provis JM. Early focal expression of the chemokine Ccl2 by Müller cells during exposure to damage-inducing bright continuous light. *Invest Ophthalmol Vis Sci.* 2011;52: 2379–2388.
34. Natoli R, Zhu Y, Valter K, Bisti S, Eells J, Stone J. Gene and noncoding RNA regulation underlying photoreceptor protection: microarray study of dietary antioxidant saffron and photobiomodulation in rat retina. *Mol Vis.* 2010;16:1801–1822.
35. Ashburner M, Ball CA, Blake JA, et al. Gene ontology: tool for the unification of biology. The Gene Ontology Consortium. *Nat Genet.* 2000;25:25–29.
36. Dennis G Jr, Sherman BT, Hosack DA, et al. DAVID: Database for Annotation, Visualization, and Integrated Discovery. *Genome Biol.* 2003;4:P3.
37. Bruford EA, Lush MJ, Wright MW, Sneddon TP, Povey S, Birney E. The HGNC Database in 2008: a resource for the human genome. *Nucleic Acids Res.* 2008;36:D445–D448.
38. Rozen S, Skaletsky H. Primer3 on the WWW for general users and for biologist programmers. *Methods Mol Biol.* 2000;132:365–386.
39. Chen L, Wu W, Dentchev T, et al. Light damage induced changes in mouse retinal gene expression. *Exp Eye Res.* 2004;79:239–247.
40. Cornish EE, Madigan MC, Natoli R, Hales A, Hendrickson AE, Provis JM. Gradients of cone differentiation and FGF expression during development of the foveal depression in macaque retina. *Vis Neurosci.* 2005;22:447–459.
41. Maslim J, Valter K, Egensperger R, et al. Tissue oxygen during a critical developmental period controls the death and survival of photoreceptors. *Invest Ophthalmol Vis Sci.* 1997;38:1667–1677.
42. Wong GW, Wang J, Hug C, Tsao TS, Lodish HF. A family of Acrp30/adiponectin structural and functional paralogs. *Proc Natl Acad Sci U S A.* 2004;101:10302–10307.
43. Joly S, Francke M, Ulbricht E, et al. Cooperative phagocytes: resident microglia and bone marrow immigrants remove dead photoreceptors in retinal lesions. *Am J Pathol.* 2009;174:2310–2323.
44. Charlesworth JA, Williams DG, Sherington E, Lachmann PJ, Peters DK. Metabolic studies of the third component of complement and the glycine-rich beta glycoprotein in patients with hypocomplementemia. *J Clin Invest.* 1974;53:1578–1587.
45. Kaneko H, Nishiguchi KM, Nakamura M, Kachi S, Terasaki H. Characteristics of bone marrow-derived microglia in the normal and injured retina. *Invest Ophthalmol Vis Sci.* 2008;49:4162–4168.
46. Davoust N, Vuaillat C, Androdias G, Nataf S. From bone marrow to microglia: barriers and avenues. *Trends Immunol.* 2008;29:227–234.
47. Zimmer B, Hartung HP, Scharfenberger G, Bitter-Suermann D, Hadding U. Quantitative studies of the secretion of complement component C3 by resident, elicited and activated macrophages: comparison with C2, C4 and lysosomal enzyme release. *Eur J Immunol.* 1982;12:426–430.
48. Lappin D, Hamilton AD, Morrison L, Aref M, Whaley K. Synthesis of complement components (C3, C2, B and C1-inhibitor) and lysozyme by human monocytes and macrophages. *J Clin Lab Immunol.* 1986;20:101–105.
49. Einstein LP, Hansen PJ, Ballow M, et al. Biosynthesis of the third component of complement (C3) in vitro by monocytes from both normal and homozygous C3-deficient humans. *J Clin Invest.* 1977; 60:963–969.
50. Walker DG, Kim SU, McGeer PL. Complement and cytokine gene expression in cultured microglial derived from postmortem human brains. *J Neurosci Res.* 1995;40:478–493.
51. Cole DS, Morgan BP. Beyond lysis: how complement influences cell fate. *Clin Sci (Lond).* 2003;104:455–466.
52. Chang CJ, Cherng CH, Liou WS, Liao CL. Minocycline partially inhibits caspase-3 activation and photoreceptor degeneration after photic injury. *Ophthalmic Res.* 2005;37:202–213.
53. Ni YQ, Xu GZ, Hu WZ, Shi L, Qin YW, Da CD. Neuroprotective effects of naloxone against light-induced photoreceptor degeneration through inhibiting retinal microglial activation. *Invest Ophthalmol Vis Sci.* 2008;49:2589–2598.
54. Gasque P, Neal JW, Singhrao SK, et al. Roles of the complement system in human neurodegenerative disorders: pro-inflammatory and tissue remodeling activities. *Mol Neurobiol.* 2002;25:1–17.
55. Nissen MH, Röpke C, Fischbarg J. Innate and adaptive immunity of the eye. *Advances in Organ Biology.* Amsterdam: Elsevier; 2005: 291–305.
56. Mallam JN, Hurwitz MY, Mahoney T, Chevez-Barrios P, Hurwitz RL. Efficient gene transfer into retinal cells using adenoviral vectors: dependence on receptor expression. *Invest Ophthalmol Vis Sci.* 2004;45:1680–1687.
57. Mevorach D, Mascarenhas JO, Gershov D, Elkon KB. Complement-dependent clearance of apoptotic cells by human macrophages. *J Exp Med.* 1998;188:2313–2320.
58. Takizawa F, Tsuji S, Nagasawa S. Enhancement of macrophage phagocytosis upon iC3b deposition on apoptotic cells. *FEBS Lett.* 1996;397:269–272.

59. Rohrer B, Demos C, Frigg R, Grimm C. Classical complement activation and acquired immune response pathways are not essential for retinal degeneration in the rd1 mouse. *Exp Eye Res.* 2007;84:82–91.
60. Jensen ML, Honore C, Hummelshoj T, Hansen BE, Madsen HO, Garred P. Ficolin-2 recognizes DNA and participates in the clearance of dying host cells. *Mol Immunol.* 2007;44:856–865.
61. Johnston RB Jr. The complement system in host defense and inflammation: the cutting edges of a double edged sword. *Pediatr Infect Dis J.* 1993;12:933–941.
62. Rambach G, Wurzner R, Speth C. Complement: an efficient sword of innate immunity. *Contrib Microbiol.* 2008;15:78–100.
63. van Beek J, Elward K, Gasque P. Activation of complement in the central nervous system: roles in neurodegeneration and neuroprotection. *Ann N Y Acad Sci.* 2003;992:56–71.
64. Harboe M, Ulvund G, Vien L, Fung M, Mollnes TE. The quantitative role of alternative pathway amplification in classical pathway induced terminal complement activation. *Clin Exp Immunol.* 2004;138:439–446.
65. Rohrer B, Coughlin B, Kunchithapautham K, et al. The alternative pathway is required, but not alone sufficient, for retinal pathology in mouse laser-induced choroidal neovascularization. *Mol Immunol.* 2011;48:e1–8.
66. Rapp L, Naash M, Wiegand R, et al. Morphological and biochemical comparisons between retinal regions having differing susceptibility to photoreceptor degeneration. In: LaVail MM, Hollyfield JG, Anderson RE, eds. *Retinal Degeneration: Experimental and Clinical Studies*. New York: Alan R Liss, Inc.; 1985;421–437.
67. Karagianni N, Adamis AP. The case for complement and inflammation in AMD: open questions. *Adv Exp Med Biol*. 2010;703:1–7.
68. Johnson PT, Betts KE, Radeke MJ, Hageman GS, Anderson DH, Johnson LV. Individuals homozygous for the age-related macular degeneration risk-conferring variant of complement factor H have elevated levels of CRP in the choroid. *Proc Natl Acad Sci U S A.* 2006;103:17456–17461.
69. Gupta N, Brown KE, Milam AH. Activated microglia in human retinitis pigmentosa, late-onset retinal degeneration, and age-related macular degeneration. *Exp Eye Res.* 2003;76:463–471.
70. Patel M, Chan CC. Immunopathological aspects of age-related macular degeneration. *Semin Immunopathol.* 2008;30:97–110.
71. Ezzat MK, Hann CR, Vuk-Pavlovic S, Pulido JS. Immune cells in the human choroid. *Br J Ophthalmol.* 2008;92:976–980.
72. Penfold PL, Killingsworth MC, Sarks SH. Senile macular degeneration: the involvement of giant cells in atrophy of the retinal pigment epithelium. *Invest Ophthalmol Vis Sci.* 1986;27:364–371.
73. Cherepanoff S, McMenamin P, Gillies MC, Kettle E, Sarks SH. Bruch's membrane and choroidal macrophages in early and advanced age-related macular degeneration. *Br J Ophthalmol.* 2009; 94:918–925.
74. Dunaief JL, Dentchev T, Ying GS, Milam AH. The role of apoptosis in age-related macular degeneration. *Arch Ophthalmol*. 2002;120: 1435–1442.
75. Seddon JM, Reynolds R, Maller J, Fagerness JA, Daly MJ, Rosner B. Prediction model for prevalence and incidence of advanced age-related macular degeneration based on genetic, demographic, and environmental variables. *Invest Ophthalmol Vis Sci.* 2009;50: 2044–2053.
76. Francis PJ, Hamon SC, Ott J, Weleber RG, Klein ML. Polymorphisms in C2, CFB and C3 are associated with progression to advanced age related macular degeneration associated with visual loss. *J Med Genet.* 2009;46:300–307.
77. Klein ML, Ferris FL 3rd, Francis PJ, et al. Progression of geographic atrophy and genotype in age-related macular degeneration. *Ophthalmology*. 117:1554–1559, e1551.